24th COBEM - 2017

24th ABCM International Congress of Mechanical Engineering
December 3-8, 2017, Curitiba, PR, Brazil

COBEM-2017-1202
LOWER LIMB PROSTHESIS TO ANKLE ADAPTER MANUFACTURED IN 3D PRINTER

Patricia Macedo
Wesley Beserra
patriciacamposmacedo@gmail.com
wesley_beserra14@hotmail.com

Denner Guilhon
dennerguilhon@gmail.com

Flavio Nunes Pereira
Universidade Estadual do Maranhão, Department of Mechanical Engineering and Production Engineering, São Luis, Brazil
flaviomecn@yahoo.com.br

Abstract. *This paper aims to provide a low cost solution for the manufacture of lower limb prosthesis adapter, due to the high market value. Simulations were performed in the Inventor software and compression tests on samples made in 3D printer whose configurations are in agreement with the orthogonal distribution of Taguchi. We applied loads of 300N, 1000N and 3000N in both the simulation and the compression tests. The highest deformations were of 0.07898mm and 0.449587mm for simulations and compression tests, respectively. The simulated safety factor was 15 and the minimum load leading to the formation of cracks and settling was 13505.3N. These values satisfy a maximum deformation limit of 3mm for the mentioned loads, indicating that 3D printing is a reliable way of manufacture such components.*

Keywords: *3D printer, simulation, adapter, prosthesis, Taguchi.*

1. INTRODUCTION

The need for low cost products in prosthetics has become increasingly visible, because people with low family income, among other socioeconomic factors, show a high risk for amputation, even presenting twice as many chances to suffer amputations (DOS REIS, 2012). Health conditions such as Diabetes Mellitus account for approximately 40% of lower limb amputations, followed by auto accidents, which account for about 32.76% of that kind of amputation, as well as the consequences of congenital diseases and accidents in general (ESTEVAO, 2009). It is still more relevant that 77.3% of the elderly with any deficiencies present lower limb amputation, right or left, at different levels (VALENÇA, 2017).

Prosthesis' manufacture is usually divided in modules, and its components can be produced in aluminum, steel or titanium, among other materials (SANTOS, 2012). With the objective of provide more comfort and make production easier, in 1912 the use of aluminum instead of steel was proposed for the first time in the manufacture of prostheses (SAMPOL, 2009). These objectives draw efforts until today to the development of low-cost materials that show better results. Some of these studies focus on the application or creation of materials, whereas others are concerned with the methods of confection, taking into account the time, cost and ease of production. Rapid prototyping printers has been extensively used to this end. This kind of equipment has been widely adopted in the industry since it is able to produce a physical object directly from a CAD model (CHEN, 2003).

This kind of bioengineering application increased in recent years, although there are few works specifically on lower limb prostheses. Most of published work focuses at the construction of upper limb prostheses, mainly hand and forearm, which have already been thoroughly studied (LOPES, 2014). The present work aims to evaluate the feasibility of using a 3D printed for lower limb prosthesis to ankle adapter. To do this, we intend to compare the simulated results, obtained using the Inventor software, to those acquired through a compression test.

2. EXPERIMENTAL PROCEDURE

Considering the use of this connection by a person weighing 60 kg, it was established that each connection should support approximately 50% of the total load, since the load is distributed almost equally between each leg (RIBEIRO, 2010). Another relevant factor is the limit of deformation defined as acceptable when applying a load, which was 1cm, since this is the average length difference between the legs of a healthy individual (HOPPENFELD et al., 2002).

The experiments were based on the connection model already available in the market, as it can be seen in Figure 1(a), its installation can be done both top and bottom of the transfer, according to Figure 1(b).

Figure 1: Adapter model for lower limb prosthesis. (a) Adapter or Connection for prosthesis. (b) Installation example of the connection between the lower point of the transfer and the prosthesis foot.

The part shown in Fig 2 (a) was designed and drawn in the Inventor software to resemble the part of Figure 1 (a). According to Figure 2 (b) it is possible to perceive the two entries, the upper one for the prosthesis foot fitting, which also uses lateral screws for fixing, and the lower one that serves for fixing the transfer, which is usually threaded or uses clamp-type adapters, as can also be seen in Figure 1 (a).

Figure 2: Simulated adapter model for lower limb prosthesis. (a) Model created in Inventor; (b) Outline of the simulated model, showing the two existing entries, one for the prosthesis foot and the other for the transfer fitting.
Adapter model for lower limb prosthesis.

Considering that in static position each leg supports approximately half of the weight each, a person of 60Kg will have the distributed load of 30Kg for each leg. Therefore the connection must withstand the load of approximately 300N without suffering significant deformations. The software was used to perform stress simulations to determine if the model was able to withstand a minimum load of 300N without deforming more than 3mm. For the purpose of a safety factor, simulations were also performed for the 1000N and 3000N loads.

Since the software cannot simulate fill variations, working only with solid parts, or other factors determined for the tests by the orthogonal method of Taguchi, the values obtained in the simulation were used as the basis for printing the physical models and to determine if the actual values satisfied the simulation.

For the experiments, three parameters were defined: fill percentage, number of external rings arranged at the beginning of the print and thickness (height between layers). Following the orthogonal distribution of Taguchi (Fig. 3), the four configurations, with three samples each, were printed on a Cliver 3D printer as shown in Figure 4 (a), and all were subjected to the compression test performed by a machine of the EMIC universal line DL1000, according to Figure 4 (b).

Table1: Taguchi orthogonal distribution (L3).

NUMBER OF EXPERIMENTS	COLUMN		
	1	2	3
1	1	1	1
2	1	2	2
3	2	1	2
4	2	2	1

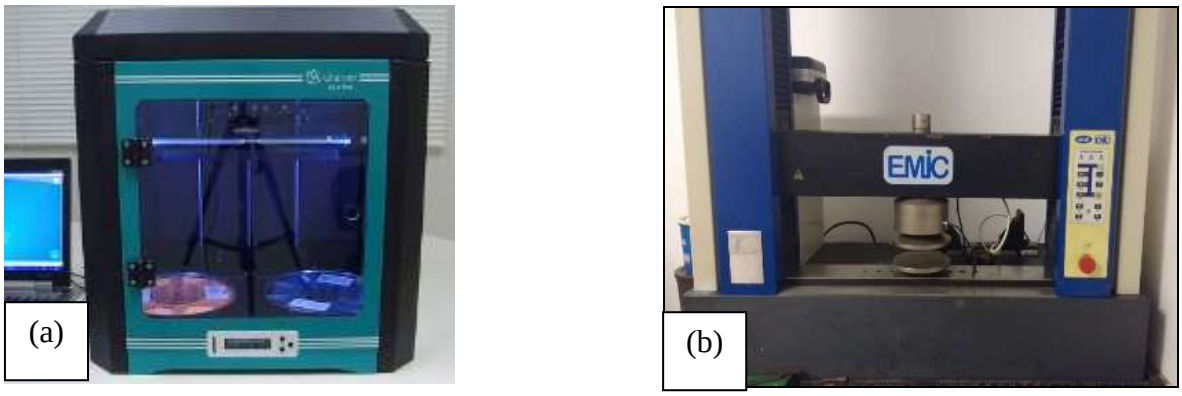

Figure 3: (a) Cliever 3D printer. (b) EMIC universal testing machine, model DL1000.

The configurations given in Figure 1 relate to the variations of each previously determined parameter, as shown in Table 2. The values were chosen according to specifications of the 3D printer, which did not allow changing parameters at random. Therefore, it was only necessary to use values of density, number of external rings and thickness already allowed by the equipment.

The compression test had a deformation of 4mm as stop parameter, applied at a speed of 0.5mm/min. Even though a test was not performed with the standard test specimen, the objective was to verify which load the connection supported until the moment of the fracture.

Table 2: Configurations specifications for the orthogonal distribution of Taguchi.

	CONFIGURATION		
TEST	DENSITY	NUMBER OF EXTERNAL RINGS	THICKNESS
111	50%	4	0,10 mm
212	25%	4	0,19 mm
221	25%	2	0,10 mm
122	50%	2	0,19 mm

To obtain the answers to the Taguchi experiment, only results obtained with the application of 3000N of load were used, for that is the safety value defined. Using the Minitab program we calculate the values of the signal-to-noise ratio (S/N), for the smaller-the-better definition, given by Eq (1). This definition was chosen due to the need for the deformation to be minimal at the time of load application.

$$10 \times \log\left(\frac{1}{n} \times \sum_{i=1}^{n} Y^2 \right) \tag{1}$$

where n is the number of experiments and Y are the values obtained in each of the experiments. In this work, three samples were used for each configuration.

3. RESULTS

The maximum deformations found for the application of 300N, 1000N and 3000N were 0.008021mm (Fig.4 (a)), 0.02681mm (Fig.4 (b)) and 0.07898mm (Fig.4 (c)) respectively . The point of greatest deformation is the same for the three simulations, which is the region of smaller cross-section, as seen in Figure 4, since this area suffers the greatest tension and is more prone to deformation.

Following the information in Table 2 and the model created in the simulation software (Fig. 2 (b)) the parts were 3D printed, with three samples each, as shown in Figure 5 (a). In total, 12 experiments were carried out. The infill differences (50% and 25%) can be visualized in Figure 5 (b), which highlighted the final deformation results.

The compression test was performed with a stop criterion of 4mm deformation. Using the data generated by this test it was possible to find the deformations for the pre-established loads. Since each configuration had three samples, the results presented are the arithmetic mean, as can be seen in Table-3.

Table 3: Average deformation of each configuration when subjected to loads of 300N, 1000N and 3000N.

	CONFIGURATION			AVERAGE DEFORMATION (mm)		
TEST	**DENSITY**	**NUMBER OF EXTERNAL RINGS**	**THICKNESS**	**300N**	**1000N**	**3000N**
111	50%	4	0,10 mm	0,10452	0,172907	0,307207
212	25%	4	0,19 mm	0,11738	0,21969	0,449587
221	25%	2	0,10 mm	0,1118	0,199293	0,415527
122	50%	2	0,19 mm	0,06462	0,154237	0,36181

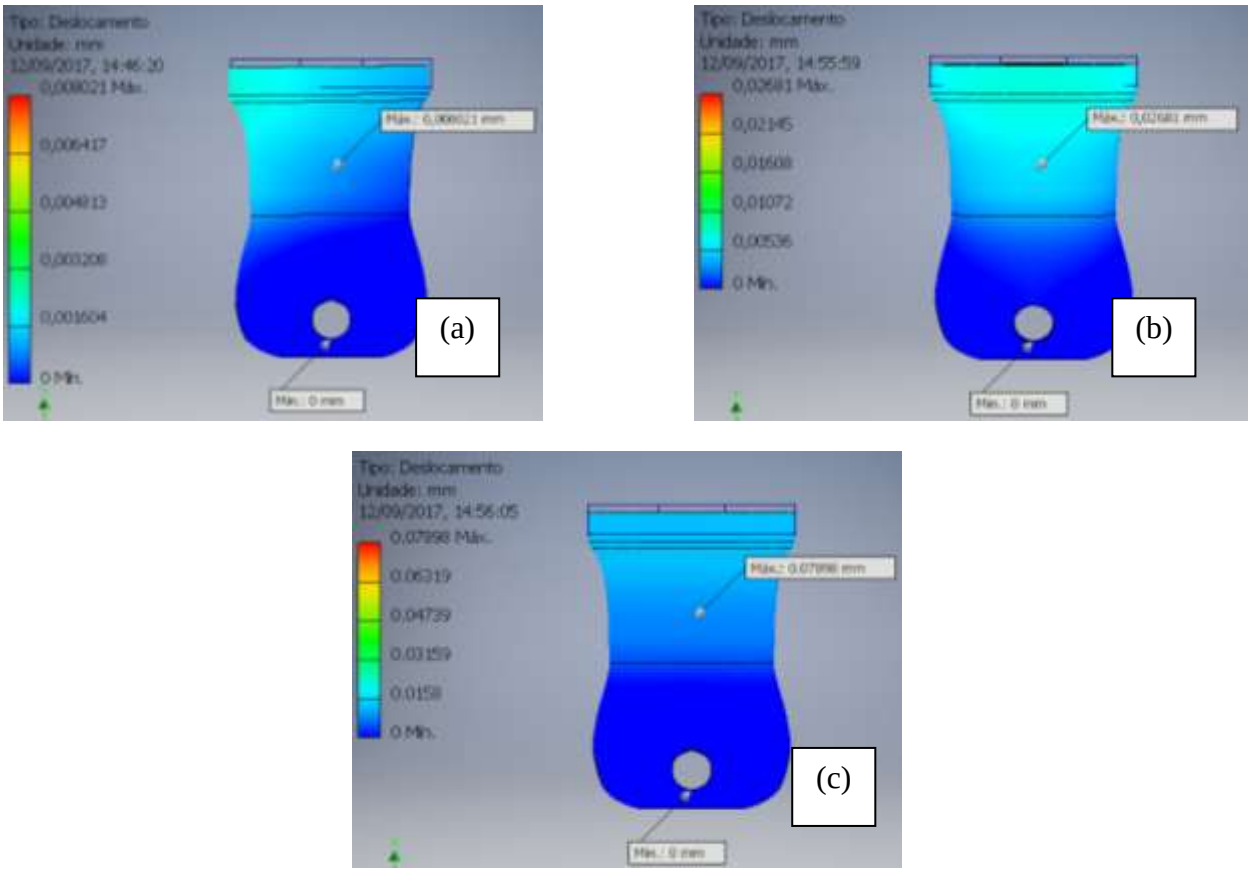

Figure 4: Simulation of the deformation for the application of (a) 300N; (b) 1000N and (c) 3000N.

.

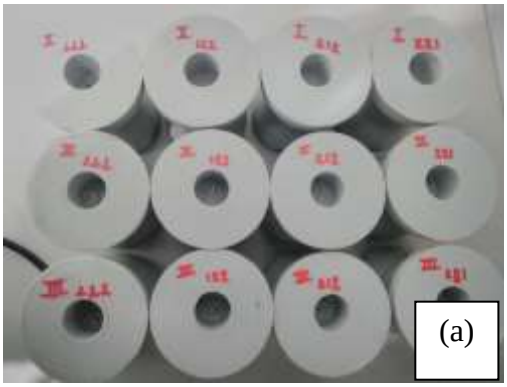

Figure 5: (a) Models 3D printed with their triples according to the orthogonal distribution of Taguchi (L3). (b) Upper and lower parts with 50% and 25% fill, respectively.

In order to analyze the individual impact of the factors, defined in Table 2, it is necessary to verify the values of the signal-to-noise ratio (S / N) that were obtained in Minitab, according to Table-4. The density factor, represented by column A, presented the largest difference between ratios, about 2,205, while the factor of column B, external layers, has the smallest difference in value, about 0.342.

Table 4: Data adapted from Minitab, showing the difference (Delta) between the ratios (S / N). Factors A, B and C, respectively, are the density, outer layers and thickness

Response Table for Signal-to-Noise Ratios

Smaller the Better

Level	**A**	**B**	**C**
1	9.489	8.557	8.899
2	7.283	8.215	7.873
Delta	**2.205**	**0.342**	**1.027**

The cost of material to manufacture these models did not exceed R$ 13.00 (thirteen Reals) per unit, as shown in Table 5.

Table-5: Quantity in millimeters, cost and printing time to manufacture each configuration.

	CONFIGURATION					
MODEL	**DENSITY**	**NUMBER OF EXTERNAL RINGS**	**THICKNESS**	**FILAMENT (mm)**	**COST (R$)**	**TIME**
111	50%	4	0,10 mm	23472	12,82	10:56:22
212	25%	4	0,19 mm	16158	8,33	06:23:07
221	25%	2	0,10 mm	14517	7,92	06:58:25
122	50%	2	0,19 mm	21504	11,73	08:28:16

4. DISCUSSION

The deformations found in the simulation and in the compression test had a significant difference, according to the graph of Figure 6. This is mainly because the simulation only works with massive pieces, which results in a greater

resistance to deformation, while the models used in the experiments were only 50% and 25% filled, so they could be considered more fragile and therefore suffered greater deformations.

Figure 6: Average deformation plot as a function of force, for each of the configurations and for the simulation.

The experiment performed following the Taguchi distribution and the definition of *smaller-the-better* must be evaluated by the results of deformation. The most striking factor was density, which presented a difference of 2,205 (Table 4) and the most pronounced values of deformation (compare the results of 111 and 122, both with 50%, to those of 212 and 221, both with 25%, in the Table 5). As expected, varying between these two levels, from 25% to 50%, we achieve greater resistance to deformation. The configuration 111 showed less deformation for this experiment. It has 50% fill, 4 rows of outer layer and 0.10mm of thickness.

This configuration was part of the experiments already performed, so there was no need for a confirmation experiment. In Figure 7 it can be seen that the configuration 111 actually showed the least deformation for the application of 3000N of load.

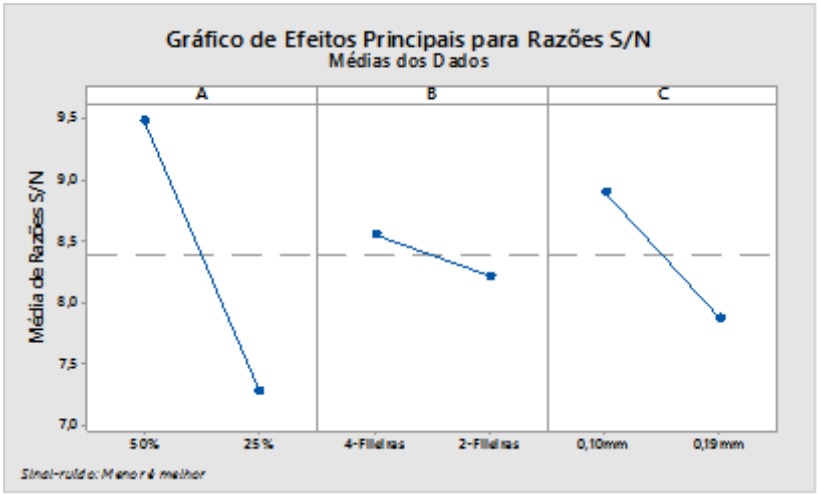

Figure 7: Impact of each factor to achieve the smaller deformation possible under the application of 3000N load. Factor A corresponds to density, B to the number of external rings and factor C represents the thickness.

We have observed during tests that fractures appeared when deformation was of approximately 4mm and that at this point the parts started to bulge. In Table-6 we find the average load values under which cracks first appeared in the parts, indicating values much higher than those specified by our design needs, assuring the reliability of all four models.

Table-6: Average load reached by each configuration at which parts suffered cracks and started to bulge.

	CONFIGURATION			
TEST	**DENSITY**	**NUMBER OF EXTERNAL RINGS**	**THICKNESS**	**AVERAGE LOAD (N)**
111	50%	4	0,10 mm	28141
212	25%	4	0,19 mm	15209,3
221	25%	2	0,10 mm	13505,3
122	50%	2	0,19 mm	19648,3

In Fig. 8 it is possible to visualize the formation of cracks, except for model 122, which was the only one that did not present a fracture when under 4 mm of deformation. This was possibly due to the configuration with larger spacing, because it had only two external layers and a thickness of 0.19mm (Table 2). Therefore, this may be the most flexible configuration.

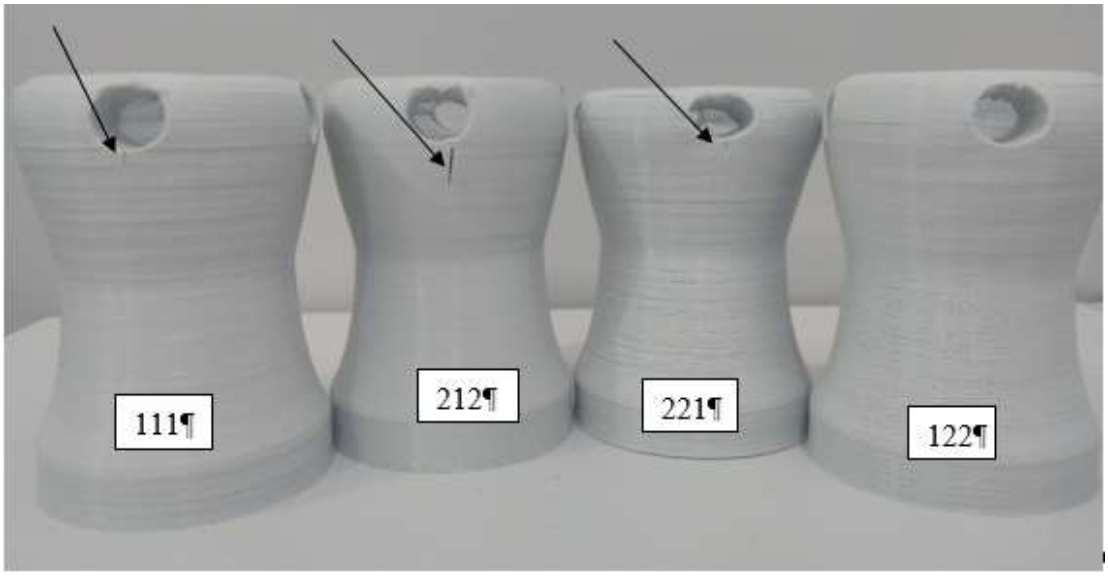

Figure 8: Emergence of cracks when a deformation of 4 mm was reached, except for the 122 model.

5. CONCLUSIONS

The deformations found in the simulation satisfy the maximum limit of 3mm, in addition to establishing a safety factor of 15 for the three loads. The results found in the compression tests had similar behavior: the configuration 111 (50%, 4 rings, 0.10mm) suffered the smallest deformation values, while configuration 212 (25%, 4 rings, 0.19mm) the greatest ones.

Which is in agreement with the result of the Taguchi experiment, given by Figure-9, in which the most efficient configuration in the smallest deformation requirement was 111. Although a test was not performed with the piece in configuration 222 (25%, 2 rings, 0.19mm), the result of 212 was already expected, since this configuration has two of the characteristics of lower performance, besides that the factor ‘external rings‘ was the one that presented the least relevance in the final results. As can be seen in Figure 7, the second column representing the ‘external rings‘ factor was the one that presented the lowest delta among the three factors used. This is therefore the least impacting factor, while the 'density' factor has the largest delta and is the most significant factor.

Despite this, the model 212 still meets the pre-requisites of maximum deformation under the load specified for the safety factor (3000N). The reliability of the models is indicated by the high load values required for cracking and bulging, which establishes that they are able to withstand, under static conditions, the maximum safety load.

The proposed adapter design has as disadvantage its time to print, which can be eventually reduced by using slender parts. On the other hand, this adapter was not originally thought to be produced at large scale, but rather under request and in an almost personalized way, as occurs with the impression of superior member prosthesis by NGOs (RIBEIRO, 2016).

6. ACKNOWLEDGMENTS

This work was technically supported by the Automation and Control Group – NAuCo/UEMA and had entire financial funding from FAPEMA under grant Universal Project 00759/15.

7. REFERENCES

CHEN, Y. H.; NG, C. T. Integrated reverse engineering and rapid prototyping. Computers & Industrial Engineering, v. 33, n. 3-4, p. 481-484, 1997 apoud ULBRICH, Cristiane Brasil Lima et al. Engenharia reversa e prototipagem rapida. 2003.

DOS REIS, Gleycykely; JÚNIOR, Adroaldo José Casa; DA SILVEIRA CAMPOS, Rodrigo. Perfil epidemiológico de amputados de membros superiores e inferiores atendidos em um centro de referência,2012.

ESTEVAO, Ricardo Jorge Oliveira. Desenvolvimento de uma prótese transtibial endoesquelética. 2009. Dissertação de Mestrado. Universidade de Aveiro.

HOPPENFELD, S.; QUADRA, A. A. F.; VIZEU, I. M. X. Propedêutica Ortopédica: coluna e extremidades. São Paulo: Atheneu, 2002.

LOPES, Jeferson Andris Lima; ALMEIDA, Lucas Coelho. Metodologia para concepção de prótese ativa de mão utilizando impressora 3d. 2014.

RIBEIRO, Ana Paula. Avaliação estática do complexo tornozelo-pé e padrões dinâmicos da distribuição da pressão plantar de corredores com e sem fasciite plantar. Tese de Doutorado. Universidade de São Paulo, 2010.

RIBEIRO, William Cândido; MIYADAIRA, Alberto Noboru; FERRUZZI, Yuri. DESENVOLVIMENTO DE MÃO ROBÓTICA DE BAIXO CUSTO. Revista Eletrônica Científica Inovação e Tecnologia, v. 1, n. 13, p. 93-99, 2016.

SAMPOL, D.A.V., A Protetização no Amputado de Membro Inferior, in Fisio&Terapia, 2000 apoud ESTÊVÃO, Ricardo Jorge Oliveira. Desenvolvimento de uma prótese transtibial endoesquelética. 2009. Dissertação de Mestrado. Universidade de Aveiro.

SANTOS, Isabel Cristina Ramos Vieira et al. Amputations for diabetic foot and social factors: implications for nursing preventive care. Northeast Network Nursing Journal, v. 12, n. 4, 2012.

VALENÇA, Tatiane Dias Casimiro et al. Repercussões sociais da aquisição de uma deficiência física na vida de idosos. Kairós Gerontologia. Revista da Faculdade de Ciências Humanas e Saúde. ISSN 2176-901X, v. 20, n. 1, p. 41-55, 2017.

8. RESPONSIBILITY NOTICE

The authors are the only responsible for the printed material included in this paper.